



Multi-criteria design of undersea arch-type structures using shape parameterization

Waldemar H. LLamosas-Mayca^{1,*}, Eugenio Lorente-Ramos³, Alejandro M. Hernández-Díaz², Jorge Pérez-Aracil³, Manuel D. García-Román¹, Sancho Salcedo-Sanz³

ARTICLE INFO

Article history:

Received 15 Mar 2026;
in revised from 24 Mar 2026;
accepted 25 Apr 2026.

Keywords:

Marine infrastructures, Submerged arches, Shape parameterization, Machine learning, Surrogate models.

ABSTRACT

The increasing need for infrastructure to solve communication problems between territories motivates the development of new techniques to find the better solution, taking into account technical, economic, safety and serviceability criteria. One of the most used structural type to design submerged structures has been the arches, which design involves several variables to meet the aforementioned requirements. The design of such structures was traditionally focused in their funicular or moment less shapes. Past works, shown that for intermediate depth ratios, the funicular shape of a submerged arch has a form between the ellipse and parabola conic curves. Later, some authors have proposed to involve in the design of these structures other aspects as the enclosed airspace to improve their serviceability, in addition to the arches mechanical behavior. For this purpose, they proposed to parameterize the curves that defined the shapes of the submerged arches and use metaheuristics to find the shape of the most appropriate solution for the submerged arches according with these criteria. These processes traditionally also require the implementation of a finite element model and the corresponding parametric function to evaluate the mechanical behavior of these structures. Since this process may be greatly simplified by using machine learning, this opens a new path to be considered in the design of these types of structures. In this work, the methodologies to design submerged arches type structures are presented. To this aim, three different parametric functions are considered: conics, elliptics and Bézier curves, and a proposal of surrogate model are presented.

© SEECMAR | All rights reserved

1. Introduction.

Arches are a type of structures that can support loads in which the internal resistance is provided mainly by their geometry[16]. In this sense, the submerged arches were traditionally

underwater installations designed pointing to funicular or momentless structure type.

Some works in the last years proposed a linear combination of conic curves (in particular, ellipse and parabola) for defining the shape of submerged arches[8] with the minimal bending moments (close to the funicular condition) and the maximum enclosed airspace (to improve their serviceability conditions).

In this work, a methodology is proposed in addition to the traditional funicular focus for the design of submerged arch-type marine structures based on shape parameterization and machine learning. For this purpose, the arch's shapes have been defined using parameterizations based on conic parabola-ellipse, elliptic, and Bézier curves. Furthermore, a database has been created for each parameterization, containing the values of the individuals that define each arch and their corresponding fitness

¹Department of Civil, Nautical and Marine Engineering, University of La Laguna, Planta baja. Vía Auxiliar de Paso Alto, 2, Santa Cruz de Tenerife, 38200, Santa Cruz de Tenerife, Spain.

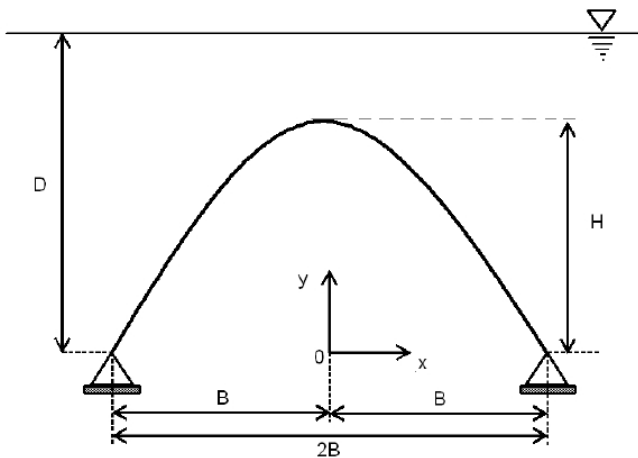
²Department of Continuum Mechanics and Structural Analysis, University of La Laguna, Ángel Guimerá Jorge 1, San Cristóbal de La Laguna, 38206, Santa Cruz de Tenerife, Spain.

³University of Alcalá, Ctra.Madrid-Barcelona, km 33, Alcalá de Henares, 28805, Madrid, Spain.

*Corresponding author: Waldemar H. LLamosas-Mayca. E-mail Address: wllamosa@ull.edu.es.

values, in order to develop the surrogate model.

Figure 1: Coordinate system and geometry of a submerged arch.



Source: Authors.

2. Funicular approach design.

For this analysis, a symmetrical submerged arch has been used. Its scheme and coordinate system are shown in Fig. (1), where the distance between the supports or the span is $2B$, the height of the arch is H measured on the axis of symmetry and the distance between the surface of the water and the line of supports is D .

2.1. Funicular equilibrium.

Funicular or momentless arches are those in which the internal forces resultant is only a single normal force in any cross section perpendicular to its guideline.

The funicular guideline of a submerged arch due to its self-weight and the effect of the hydrostatic pressure acting on it is defined by the expression: $y(x)$ [8]. The equation of $y(x)$ is obtained by solving the Eq. (1) and applying the boundary conditions. This equation is the result of applying the equilibrium conditions to the free body diagram shown in Fig. (2) and can be solved by numerical integration methods such as Runge-Kutta or Euler[2, 9, 8].

$$\frac{dN}{dx} = \frac{N\gamma_s}{\sigma_o} \frac{dy}{dx}$$

$$\frac{d^2y}{dx^2} = -\left[\frac{\gamma_w(D-y(x))}{N} + \frac{\gamma_s}{\sigma_o} \left(1 + \left(\frac{dy}{dx} \right)^2 \right)^{-1/2} \right] \left(1 + \left(\frac{dy}{dx} \right)^2 \right)^{3/2}$$

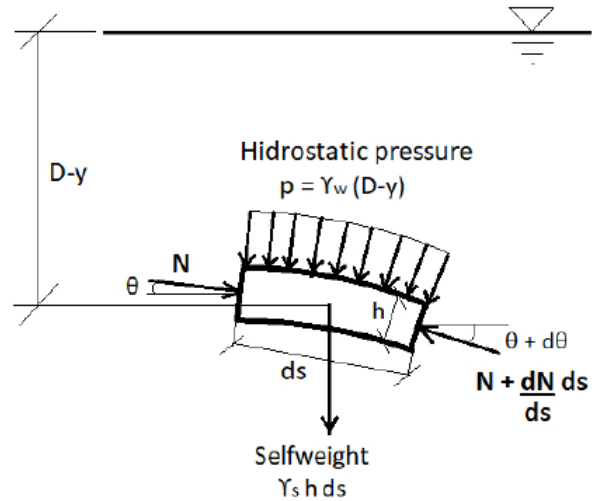
$$\frac{dy}{dx} \Big|_{x=0} = 0$$

$$y(0) = H; \quad N(0) = \sigma_o h$$

(1)

In Eq. (1) $N(0)$ refers to the axial compressive force and at the apex of the arch, h to the thickness of the arch. In addition, σ_o is the compressive stress in the cross section of the arch

Figure 2: Differential element forces equilibrium.



Source: Authors.

under a fully stressed condition, γ_w is the unit weight of the water and γ_s is the unit weight of the arch's material.

It is important to emphasize that according to [18], given certain conditions of depth of the support line D , height of the arch H and thickness of the arch at the apex h , the funicular arch only exists if it is subjected to a compressive force greater than a minimum value N_{min} to maintain the funicular equilibrium indicated in eq. (1), or that there may be more than one funicular arch as a solution to the proposed problem.

3. Methodological approaches for multicriteria design.

In this section, the multicriteria design of submerged arches is presented using a Finite Element Analysis (FEM) model and a Surrogate model.

For this purpose, a set of simulations have been carried out considering the geometrically linear finite element analysis of the arches structures, using parameterizations corresponding to the parabola-ellipse, Bézier and elliptical curves to define the shape of the arches. At the same time, a database with the values of the individuals used to define the arches and their corresponding fitness values resulting from the process before mentioned, has been created.

3.1. The approach based in shape parameterization.

To address this approach, the following geometric conditions have been considered for all the simulations: a distance between the surface of the water and line of supports of $D = 50$ m, an arch height of $H = 6$ m., the thickness and semi-span of the arch varying in the ranges shown in the table (1), with a maximum value of $h = 5$ m. and to $B = 100$ m. respectively. The number of iterations performed to obtain a data base of at least 2000 values, has been of $n = 25$ for parabola-ellipse and Bézier simulations and $n = 35$ for elliptic parameterization.

Table 1: Linear analysis. Deep waters (D = 50 m). Individuals design parameters.

Parabola-Ellipse		Bézier		Elliptic	
Parameter	Range	Parameter	Range	Parameter	Range
H' (m)	[3.1, 100]	P_{2x} (m)	[-50, 50]	p	[-5000, -0.01]
B (m)	[0.1, 100]	P_{2y} (m)	[0, 6]	q	[0.01, 5000]
		P_{3x} (m)	[-50, 50]		
H (m)	6	P_{3y} (m)	6	H (m)	6
t	[0, 1]	P_{4x} (m)	[1.5, 100]	λ	[0.01, 10]
h (m)	[0.105, 5.0]	h (m)	[0.105, 5.0]	h (m)	[0.105, 5.0]

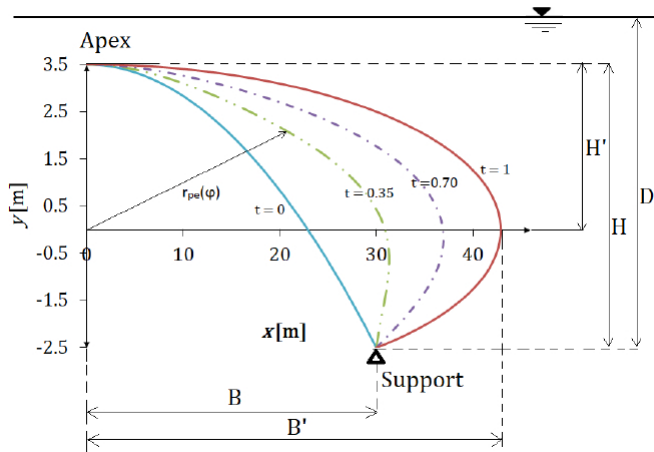
Source: Authors.

3.1.1. Parabola Ellipse curves.

This parameterization results from the linear combination of the equations that define the conic curves parabola and ellipse, and it is shown in Eq. (4) [8].

The individuals used in this parameterization are defined by the parameters B , H , H' , t , shown in Fig. (3), and h . In this definition, B is the x-coordinate of the arch' support, H is the height of the arch, B' and H' are respectively the lengths of the semi-major axis and the semi-minor axis of the ellipse, t is the parameter that defines the linear combination between both curves, and h which is the thickness of the arch at the apex.

Figure 3: Parabola Ellipse parameterization.



Source: Authors.

The polar coordinate system ($r - \varphi$) has been used to define the conic curves to avoid the errors that a numerical integration would produce if they were defined using Cartesian coordinates, caused by an infinite slope at some points of the arches [18, 17], resulting from some combinations of the parameters that define an individual.

Thus, the polar definition of the parabola r_p and the ellipse r_e according to [8], are shown in Equations (2) and (3) respectively.

$$r_p(\varphi, B, H, H') = \frac{B^2 \sec^2 \varphi \left(\sqrt{\frac{4 \cos^2 \varphi \left(1 + \frac{H-H'}{H'}\right)}{B^2} + \frac{\sin^2 \varphi}{H'^2}} - \frac{\sin \varphi}{H'} \right)}{2 \left(1 + \frac{H-H'}{H'}\right)} \quad (2)$$

$$r_e(\varphi, B', H') = \frac{1}{\sqrt{\frac{\cos^2 \varphi}{B'^2} + \frac{\sin^2 \varphi}{H'^2}}} \quad (3)$$

Consequently, a set of values B , H , H' and t , completely define a curve with respect to its radial coordinate r_{pe} and its angular coordinate φ .

$$r_{pe}(t, \varphi, B, H, H') = (1 - t) \cdot r_p + t \cdot r_e(\varphi) \quad (4)$$

[18, 17, 8]

3.1.2. Elliptic curves.

In this parameterization, Elliptic curves of third degree have been used to define the shape of the arch. For this purpose, the dimensionless parameters p , q , λ , have been fixed and replaced in Eq. (8)). The individuals are defined by these three parameters in addition to H and h , which are the height and thickness at the apex of the arch, respectively.

To define an elliptic curve, K has been considered a commutative field. Then, the elliptic curve E is an algebraic plane curve defined by the Weierstrass equation [7, 13]

$$E : y^2 + a_1xy + a_3y = x^3 + a_2x^2 + a_4x + a_6 \quad (5)$$

where $a_1, a_2, a_3, a_4, a_6 \in K$, with discriminant $\Delta \neq 0$.

The discriminant of Weierstrass Eq.(5) is:

$$\Delta = -b_2^2b_8 - 8b_4^3 - 27b_6^2 + 9b_2b_4b_6 \quad (6)$$

where:

$$b_2 = a_1^2 + 4a_2$$

$$b_4 = 2a_2 + a_1a_3$$

$$b_6 = a_3^2 + 4a_6$$

$$b_8 = a_1^2a_6 + 4a_2a_6 - a_1a_3a_4 + a_2a_3^2 - a_4^2$$

For practical purposes, the discriminant of the canonical expression can be simplified to the following, as shown in Eq. (7)

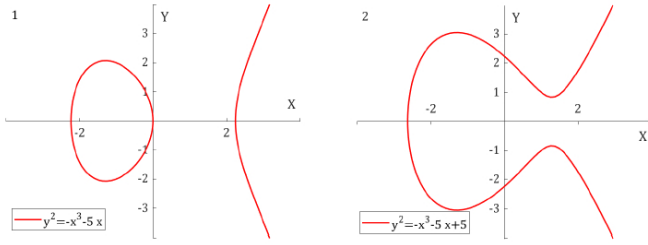
$$\Delta 1 = -4p^3 - 27q^2 \quad (7)$$

Some examples of elliptic curves are shown in Figure (4).

For our purpose of using these curves in the arches shape parameterization, it is convenient to rotate the curve a quarter turn clockwise and to operate with the expression resulting in this affine transformation. In this order, we make the substitutions $x \rightarrow -y$, $y \rightarrow x$, and the expression *canonical* of the elliptic curve is obtained Eq. (8):

$$x^2 = -(\lambda y)^3 - p\lambda y + q, \quad (8)$$

Figure 4: Graphical examples of elliptic curves. 1: elliptic curve with two components (closed oval and pseudo-line); 2: elliptic curve with only one component (pseudoline).

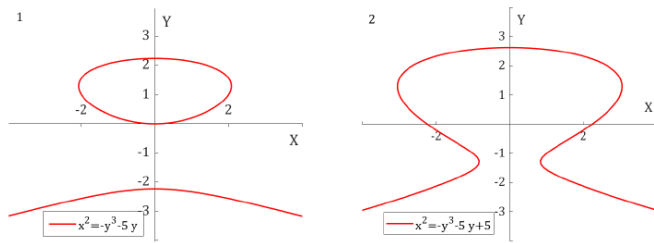


Source: Authors.

$$p, q, \lambda \in K.$$

The rotated elliptic curves resulting from Eq. (8) are shown in Figure (5).

Figure 5: Graphical examples of elliptic curves rotated. 1: elliptic curve with two components (closed oval and pseudo-line); 2: elliptic curve with only one component (pseudoline).



Source: Authors.

3.1.3. Bézier curves

Bézier curves have been used to define the geometry of the arch shape.

In this parameterization, their geometry is obtained by fixing using control points and to define the individuals, it is enough to consider the coordinates of the control points $P1 = (0, 0)$, $P2 = (p2x, p2y)$, $P3 = (p3x, p3y)$, $P4 = (p4x, p4y = p3y)$, $P5 = (p5x, p5y = p3y)$, $P6 = (p6x, p6y = p2y)$, $P7 = (2B, 0)$, shown in Fig. (6), and h which is the thickness at the apex of the arch. This consideration is valid if the axis of symmetry passes through point $P4$.

Bézier curves are polynomial curves expressed using Bernstein's polynomials that express them in a way analogous to Newton's binomial. These curves are evaluated using the Casteljau algorithm. [6]

This algorithm [6, 3] applied to the evaluation of a Bézier curve of degree n , is shown in Table (2).

Table 2: Algorithm 1. Casteljau.

1:	Input:
2:	n : Degree of the Bézier curve. Number of control points - 1
3:	$b_0, b_1 \dots b_n$: Bézier curves control points.
4:	t : Interpolation parameter, $\in [0, 1]$.
5:	Output:
6:	The point on the Bézier curve at parameter t
7:	Begin:
8:	Create a temporary list of control points:
9:	For $i=0$ to n
10:	$points[i] = b[i]$
11:	End for
12:	Perform the Casteljau's algorithm:
13:	For $r=1$ to n :
14:	For $i=0$ to $n-r$:
15:	Interpolate between the points:
16:	$points[i] = (1-t) * points[i] + t * points[i+1]$
17:	End for
18:	End for
19:	Return $points[0]$

Source: Authors.

The equations to represent a Bézier curve can be written as shown in Eq. (9):

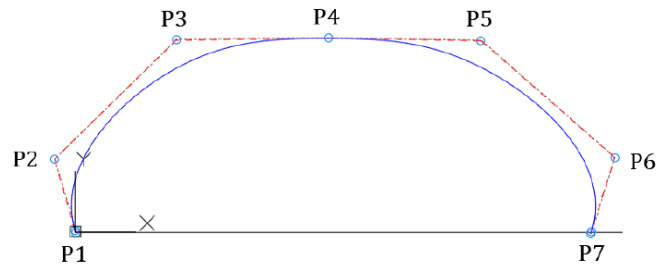
$$x(t) = \sum_{i=0}^n b_i B_i^n(t) \quad (9)$$

$$t \in [0, 1]$$

Where the Bernstein polynomials are:

$$B_i^n(t) = \binom{n}{i} (1-t)^{n-i} t^i, \text{ where, } \binom{n}{i} = \frac{n!}{(n-i)!i!} \quad (10)$$

Figure 6: Bezier parameterization control points.



Source: Authors.

3.1.4. Finite element modeling.

The geometry configuration of the arches has been defined according to the three parameterizations described above. For

each case, a geometric lineal analysis has been performed applying the hydrostatic load and its self-weight acting on them. This structural analysis has been carried out using ANSYS [15, 1] finite element software, modeling the arches with the straight element BEAM188 from ANSYS library [1], with a Young’s modulus $E = 27664,49 \cdot 10^3 kN/m^2$ and the Poisson ratio has been assumed equal to 0.3. The results of the process described above, considered for our purpose, have been the following: the values of the bending stresses, compressive stresses, and the vertical displacements of the nodes. The area of the enclosed airspace by the guidelines of the arches has also been determined. Additionally, to ensure the serviceability of the proposed arches, the maximum vertical displacement of their nodes $max(d_y)$, has been limited according to the Eq. (11) shown below:

$$\max(d_y) < B/150 \tag{11}$$

3.1.5. *Fitness function.*

To measure and compare the quality of the solutions that are being obtained, an objective or functional function is defined. In this work, that functional or fitness is calculated using the following expression:

$$f = p_m \cdot \max(|M_s|) + p_a \cdot \frac{1}{A_s} \tag{12}$$

in which p_m and p_a are, respectively, the weights of the bending stress and the enclosed area under the centerline of the arch A_s . In this work, $p_m = 0.7$ and $p_a = 0.3$ for all the cases evaluated, and $\max(|M_s|)$ represents the difference between the maximum bending moment absolute value along the arch ($|M_{max}|$) and the minimum resisting bending moment value of the arch section ($mlim$). This minimum resisting bending moment value refers to that which the arch section is capable of resisting with the minimum steel reinforcement based on the international standards prescription by [5] of the minimum concrete compressive strength and the steel reinforcement ratio in reinforced concrete members. Thus, if $|M_{max}|$ is less than $mlim$, it takes a value of zero.

3.2. *An alternative approach: surrogate models.*

The surrogate models are mathematical approximations that emulate the behavior of a system that is usually complex and usually requires a high computational burden for its exact solution. These models allow to carry out a higher number of simulations or processes in shorter time, with lower level of accuracy, but whose results may be acceptable as a solution to the problem posed. In this work, the use of surrogate models is presented to find the better solution to define the guideline of a submerged arch according to the restrictions defined before hand and evaluated using the fitness. For this purpose, a light-weight model will replace the fitness function.

This surrogate model proposed for this problem, will be implemented as a regression model that will be trained using input parameters that define the geometry of the submerged arches

and setting as the target the fitness of said arch. We will compare each of the parameterizations in order to decide which one yields a better surrogate model.

This proposal of a surrogate model for this problem, will be implemented as a regression model that will be trained using input parameters that define the geometry of the submerged arches shown in Section 3 and fixing as target, the fitness of the respective arches defined by these parameters. The results obtained for each parameterization, will be compared to identify the one that returns the most effective best surrogate model.

From the database mentioned above generated by calculating the "fitness" value of various submerged arches defined by the parameterizations mentioned in 3, a machine learning model has been trained to predict the "fitness" value of the individual which defines an arch.

The machine learning models used to implement the surrogate model proposed are presented below.

3.2.1. *Linear regression.*

The Linear regression model is a supervised learning algorithm based on the same statistical method, which approximates the data with a linear function. It is defined in Eq. (13) shown below:

$$\hat{y}(\mathbf{x}; \beta) = \beta_0 + \sum_{i=1}^{M-1} \beta_i x_i \tag{13}$$

The function $\hat{y}(\mathbf{x})$ is generated by this method and represents a M dimensional hyperplane fitted to the data. Different fitting methodologies result in a variety of linear models such as the Classic linear regression or Ridge shown below.

Classic linear regression.. In this method, the vector β for a standard linear regression model is found by selecting values that minimize the Mean Squared Error (MSE). This metric quantifies the difference between the target variable and the model predictions, as shown in Eq. (14).

$$MSE = \frac{1}{N} \sum_{i=1}^N (y_i - \hat{y}(\mathbf{x}, \beta)_i)^2 \tag{14}$$

Ridge (L2 regularization).. This is an ML technique that obtains their optimal parameters by minimizing the Ridge regression cost function E_{Ridge} Eq. (15) which comprises the MSE added to a regularization term that depends on the square of the model parameters.

$$E_{Ridge} = MSE + \alpha \sum_{i=0}^{M-1} \beta_i^2 \tag{15}$$

3.2.2. *Ensemble methods.*

In this work we are going to make use of two well known ensemble methods:

Random Forest. The Random Forest algorithm merges a set of weak models based on decision trees to create a single strong classifier [4]. For training each weak model, a random set of input variables \mathbf{x}_i is used. The result is a prediction function $h_i(\mathbf{x}_i)$. The final response of the process is generated by combining the outputs of the weak models or estimators, using the function shown in Eq. (16). The number of estimators used is M and each one has been trained as a standard desition tree.

$$f(\mathbf{x}) = \frac{1}{M} \sum_{i=0}^M h_i(\mathbf{x}_i) \quad (16)$$

3.2.3. Support Vector Machines (SVM).

The Support Vector Machines (SVM) are supervised ML models used for classification problems [12], as well as regression tasks [14]. These models have been used successfully in various domains as shown in [11]. They work by finding and building a hyperplane to separate the data into classes, which is adjusted to the training data using the tolerance margin C . The model is trained finding the value of the parameter ω that optimizes Eq. (17).

$$\omega^* = \frac{1}{2} \operatorname{argmin}_{\omega} \omega^T \omega + C + \sum_{i=1}^N (\xi_i + \xi_i^*) \quad (17)$$

In this model the kernel trick has been implemented which is a strong method to classify non-linearly separable data, and consists of transforming the space of the features with the function $\Phi(x)$ by substituting dot products with the kernel function shown in Eq. (18).

$$K(x, y) = \langle \Phi(x), \Phi(y) \rangle \quad (18)$$

In this work, the following kernels have been considered:

- Linear Kernel

$$\text{Linear Kernel: } K_{\text{linear}}(x, y) = x^T y$$

- Polynomial Kernel

$$\text{Polynomial Kernel: } K_{\text{poly}}(x, y) = (x^T y + c)^d$$

- Gaussian Kernel

$$\text{Gaussian Kernel: } K_{\text{gaussian}}(x, y) = e^{-\|x-y\|^2/2\sigma^2} = e^{-\gamma\|x-y\|^2}$$

3.2.4. Multi-layer perceptron (MLP).

The Multi-layer perceptron (MLP) is a type of artificial neural network MLPs are one of the most used ML models for classification and regression problems. It consists of a number of input nodes or neurons, that are processed by hidden layers and are passed to the output layer. Each hidden layer l consists of a set of neurons, each obtaining their value $a_{l,i}$ from the application of an activation function $\sigma(x)$ over a linear combination of the values of the previous layer added to a bias term b as shown in Eq. (19).

$$a_{l,i} = \sigma(W_{l,i} \cdot a_{l-1} + b_{l,i}) \quad (19)$$

To train this model, the weights $W_{l,i}$ and the biases $b_{l,i}$ have been fitted to minimize the error of the network's output as much as possible. The algorithm most used to perform this optimization is Stochastic Gradient Descent (SGD), which is explained in detail in [10].

3.2.5. Training of models.

As indicated in Section 3, databases were generated with the results of simulations performed with the arches defined with the parabola-ellipse, Bézier, and elliptic parameterizations, and according to the conditions indicated in Section 3.1.

The ML models mentioned above have been trained with samples coming from these databases, that contain around 2000 samples with values of the individuals used to define the arches and their corresponding fitness values (Eq. 12).

In order to carry out the training of the models, the dataset has been split into two sets, training and test set respectively. Thus, each model will be trained with a training set and evaluated with a testing set.

All data have been preprocessed, both the input and target variables, to avoid problems with the training of gradient based algorithms. This standardization of values consists of obtaining the new dataset z by subtracting from each feature c of each data point i their average value \bar{x}_c and dividing by their standard deviation σ_{x_c} as shown in Eq. (20).

$$z_{c,i} = \frac{x_{c,i} - \bar{x}_c}{\sigma_{x_c}} \quad (20)$$

To evaluate each of the models, three metrics have been used: the R2 score Eq. (21), the Root of the Mean Squared Error (RMSE) Eq. (22) and the Mean Absolute Error (MAE) Eq. (23).

We will make use of three metrics to evaluate each of the models: the R2 score Eq. (21), the Root of the Mean Squared Error (RMSE) Eq. (22) and the Mean Absolute Error (MAE) Eq. (23). The R2 score is a metric that ranges from 1 when the perfect model fit occurs and shows lower values (close to zero or negative) as the modeling differs from the real data. The MAE and RMSE scores will be non-negative values; the lower they are, the less error our model makes when approximating the original function.

$$R^2(\mathbf{y}, \hat{\mathbf{y}}) = 1 - \frac{\sum_{i=1}^N (y_i - \hat{y}_i)^2}{\sum_{i=1}^N (y_i - \bar{y})^2} \quad (21)$$

$$RMSE(\mathbf{y}, \hat{\mathbf{y}}) = \sqrt{\frac{1}{N} \sum_{i=1}^N (y_i - \hat{y}_i)^2} \quad (22)$$

$$MAE(\mathbf{y}, \hat{\mathbf{y}}) = \frac{1}{N} \sum_{i=1}^N |y_i - \hat{y}_i| \quad (23)$$

4. Results.

In this Section, the results obtained through the two approaches proposed are presented.

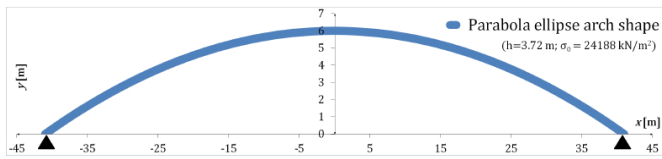
4.1. Results of the approach based in shape parameterization.

In this case, the arches have been defined using the three parameterizations mentioned above, their stresses have been obtained through an FEM, and the enclosed air space by their guidelines and fitness value have been calculated. For all cases, the search ranges are presented in Table 1 and the experiments have been performed under linear analysis according with the parameters described in Section 3.1.

- Parabola ellipse curves parameterization.

The arch was defined according to the individuals shown in Table 3 and its shape is shown in Figure 7.

Figure 7: Arch defined using Parabola Ellipse parameterization.



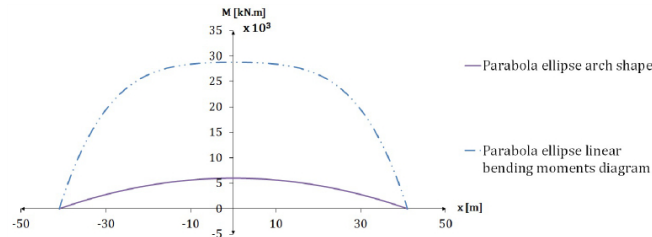
Source: Authors.

Table 3: Parabola ellipse parameterization individual.

Parabola ellipse curve individual				
H' (m)	B (m)	H (m)	t	h (m)
93.28660376	41.00146137	6	0.018661681	3.720998399

Source: Authors.

Figure 8: Arches Bending Moment Diagrams (BMD) for Parabola-Ellipse shape ($M_{max} = 28754$ kN.m, $M_{min} = 0$ kN.m).



Source: Authors.

For the simulation carried out with the Parabola ellipse parameterization, the airspace enclosed under the guideline and the fitness obtained have been $328.0211 m^2$ and 0.00091449 respectively. In addition, the maximum vertical deflection registered have been of $0.19318m$.

- Bézier curves parameterization.

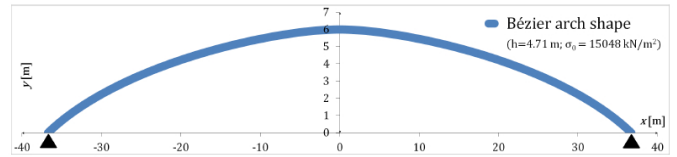
The arches were defined according to the individuals shown in Table 4 and its shape is shown in Figure 9.

Table 4: Parabola ellipse parameterization individual.

Bézier curve individual					
P_{2x} (m)	P_{2y} (m)	P_{3x} (m)	P_{3y} (m)	P_{4x} (m)	h (m)
9.274792592	4.124752378	28.88859492	6	36.72557555	4.705281187

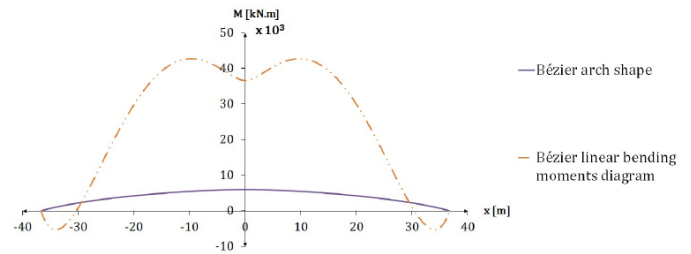
Source: Authors.

Figure 9: Arch defined using Bézier parameterization.



Source: Authors.

Figure 10: Arches Bending Moment Diagrams (BMD) for Bézier shape ($M_{max} = 42726$ kN.m, $M_{min} = 0$ kN.m).



Source: Authors.

For the simulation carried out with the Bézier parameterization, the airspace enclosed under the guideline and the fitness obtained have been $295.9377 m^2$ and 0.00101224 respectively. In this case, the maximum vertical deflection registered has been of $0.099921m$.

- Elliptic curves parameterization.

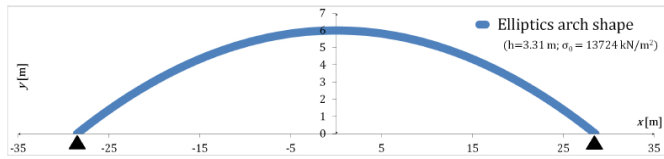
Arches were defined according to the individuals shown in Table 5 and its shape is shown in Figure (11).

Table 5: Elliptic parameterization individual.

Elliptic curve individual				
p	q	H (m)	λ	h (m)
-2563.28838	3966.995384	6	0.05282679	3.308393223

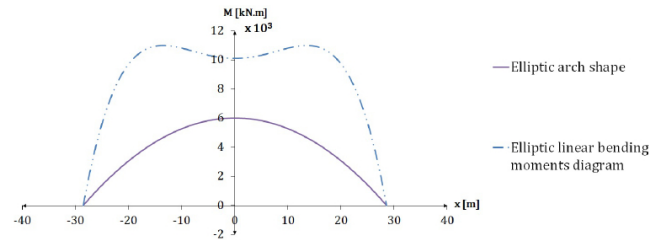
Source: Authors.

Figure 11: Arch defined using Elliptic curves parameterization.



Source: Authors.

Figure 12: Arches Bending Moment Diagrams (BMD) for Parabola-Ellipse shape ($M_{max} = 10983 \text{ kN.m}$, $M_{min} = 0 \text{ kN.m}$).



Source: Authors.

For the simulation carried out with the Bézier parameterization, the airspace enclosed under the guideline and the fitness obtained have been $228.2064m^2$ and 0.00091243 respectively. The maximum vertical deflection registered for this arch has been of $0.053611m$.

The result of the simulation carried out defining the arch with this parameterization gives a fitness value similar to the one defined with the Parabola ellipse even though the resulting semi-span is smaller.

4.2. Results of the approach based in surrogate models.

The performance of each algorithm has been compared by performing *five* cross validation repetitions with *five* splits and 10 repetitions using the training data set. Then, the average score obtained in the training splits and the validation splits have been taken and compared.

It is important to highlight that the R2 score has not been used to compare different datasets because this value depends on the average value of the target value, which is likely to differ between datasets.

From these results, for each parameterization model with the best R2 validation score was chosen and evaluated with the dataset. Then, the RMSE and MAE scores of the final models have been compared to evaluate their performance, as shown in Table 6.

Table 6: Score of the selected models for each parameterization.

Parameterization	Best Model	RMSE Test	MAE Test
Bezier curves	MLP	3.591×10^6	2.045×10^6
Elliptic curves	Random Forest	5.511×10^5	1.154×10^5
Parabola Ellipse curves	MLP	2.871×10^6	3.987×10^5

Source: Authors.

Conclusions.

In this paper, in addition to traditional methodologies used for designing optimized submerged arch-type structures, the use of surrogate models is presented. The numerical results obtained for calculating the fitness using the three proposed shape parameterizations show that the best approximation to the fitness function was obtained by modeling the arch with elliptic curves and a Random Forest model to approximate the calculations. The second-best results were obtained by defining the arch shape using Bézier curves and a regular Neural Network to approximate the fitness function. The proposed methodology based on surrogate models is able to define an optimized shape for marine submerged arch-type structures, maximizing their enclosed area and minimizing their bending moments, eliminating the need for complex finite element calculations, resulting in significant computational time savings. Future lines of research based on these results include applying this methodology to analyze the structural behavior of submerged arches type structures using a geometrically nonlinear finite element model at different depths extending the search space, as well as applying it to other types of civil engineering marine structures.”

References.

- [1] ANSYS, A., 2013. Version 15.0; ansys. Inc.: Canonsburg, PA, USA November 752.
- [2] Ascher, U.M., Petzold, L.R., 1998. Computer methods for ordinary differential equations and differential-algebraic equations. volume 61. Siam.
- [3] Boehm, W., Müller, A., 1999. On de casteljau’s algorithm. Computer Aided Geometric Design 16, 587-605.
- [4] Breiman, L., 2001. Random forests. Machine Learning 45, 5-32.
- [5] Code, P., 2005. Eurocode 2: design of concrete structures-part 1-1: general rules and rules for buildings. British Standard Institution, London 668, 659-668.
- [6] Farin, G., Hoschek, J., Kim, M.S., Kim, M.S., 2002. Handbook of Computer Aided Geometric Design. Elsevier Science I& Technology, Amsterdam. ID:311448.
- [7] Fulton, W., 2008. Algebraic curves. An Introduction to Algebraic Geom 54.
- [8] Hernández-Díaz, A.M., Bueno-Crespo, A., Pérez-Aracil, J., Cecilia, J.M., 2018. Multi-objective optimal design of submerged arches using extreme learning machine and evolutionary algorithms. Applied Soft Computing 71, 826-834.
- [9] Isaacson, E., Keller, H.B., 2012. Analysis of numerical methods. Courier Corporation.
- [10] Rumelhart, D.E., Hinton, G.E., Williams, R.J., 1986. Learning representations by back-propagating errors. Nature 323, 533-536.
- [11] Salcedo-Sanz, S., Rojo-Álvarez, J.L., Martínez-Ramón, M., Camps-Valls, G., 2014. Support vector machines in engineering: an overview. Wiley Interdisciplinary Reviews: Data Mining and Knowledge Discovery 4, 234-267.

[12] Schölkopf, B., Smola, A.J., 2002. Learning with kernels: support vector machines, regularization, optimization, and beyond. MIT press.

[13] Silverman, J.H., 2009. The arithmetic of elliptic curves. volume 106. Springer.

[14] Smola, A.J., Schölkopf, B., 2004. A tutorial on support vector regression. *Statistics and computing* 14, 199-222.

[15] Stolarski, T., Nakasone, Y., Yoshimoto, S., 2018. Engineering analysis with ANSYS software. Butterworth-Heinemann.

[16] Tadjbakhsh, I., 1981. Stability and optimum design of arch-type structures. *International Journal of Solids and Structures* 17, 565-574.

[17] Wang, C., Ler, C., 2003. Optimization of submerged funicular arches. *Mechanics Based Design of Structures and Machines* 31, 181-200.

[18] Wang, C., Wang, C., 2002. Funicular shapes for submerged arches. *Journal of Structural Engineering* 128, 266-270.